Proks et al., http://www.jgp.org/cgi/content/full/jgp.201411222/DC1

Simulations of the effect of P_O on the EC_{50} for Mg-nucleotide activation

Is the shift in EC_{50} for Mg-nucleotide activation in the presence of gliclazide produced by the reduction in P_O produced by the drug? In principle, changes in gating could account for the shift in the EC_{50} for MgADP activation produced by gliclazide (Colquhoun, 1998). To address whether this is actually the case, we must first consider the complication that Mg-nucleotide activation of Kir6.2-G334D/SUR1 channels consists of an increase in both *N* and P_O (Proks et al., 2010). Given that inactive channels have a P_O close to zero and that the mean P_O of active channels is ∼0.4, different EC_{50} values might be expected for the increase in *N* and P_O in the absence of gliclazide (Colquhoun, 1998). This would be expected to give rise to a biphasic MgADP concentration-activation curve or a slope factor of <1, depending on the relative magnitudes of the effect of MgADP on *N* and P_O. However, this was not observed (Proks et al., 2010). Furthermore, because the decline in P_O after patch excision stabilizes much earlier than that in *N*, any difference in the EC_{50} for the MgADP-induced increase in *N* and P_O would be expected to result in the development of a biphasic concentration-activation relation (or change in EC_{50} and/or in slope) after patch excision. This was also not observed (Proks et al., 2010). Thus, it appears that the EC_{50} for MgADP activation of *N* and P_O are similar or that the effect of one of them dominates. In most patches the effect on *N* and P_O was of comparable size (Proks et al., 2010), implying the EC_{50} must also be similar.

Noise analysis indicated that gliclazide reduced the ability of 1 mM MgADP to enhance the P_O of Kir6.2-G334D/SUR1 channels by ∼20% and decreased *N* by ∼60%, indicating that both activatory processes are still present in the presence of the drug. The MgADP concentration-activation relationship was monophasic, with a slope factor (*h*) similar to that in the absence of the drug. Thus, the drug is unlikely to differentially influence the EC_{50} for the activatory mechanisms governing P_O and *N*.

Collectively, these observations indicate that the increase in P_O and *N* produced by MgADP do not have markedly different EC_{50} and are not differentially affected by gliclazide. Thus, we can now consider whether gliclazide affects the gating equilibrium by focusing on the effect of the drug on the P_O of active (functional) channels. There was no obvious relationship between the mean P_O of Kir6.2-G334D/SUR1 channels measured before nucleotide application (range 0.2–0.6), and the extent of activation by an MgADP concentration close to the EC_{50} (Fig. S6 A). High-affinity gliclazide inhibition reduces P_O by a maximum of ∼60% (i.e., from 0.6 to 0.24 or from 0.2 to 0.08); because P_O over the range 0.2–0.6 has little effect on EC_{50}, it is unlikely that gliclazide substantially influences EC_{50} via changes in P_O of active channels in the membrane. In support of this idea, a concerted model of K_{ATP} channel gating (Drain et al., 2004; Babenko, 2008; Craig et al., 2008) also predicts only small changes in EC_{50} over this range of P_O (Fig. S6, B and C).

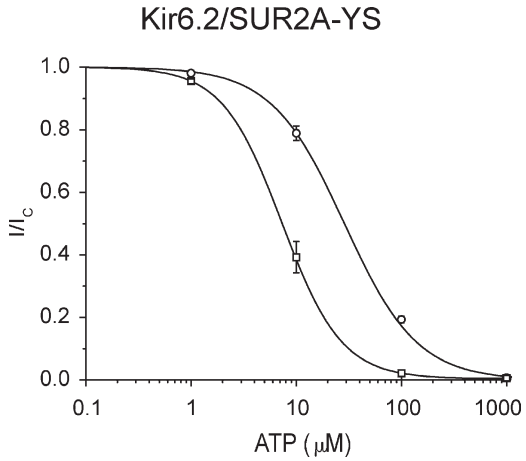

Figure S1. Concentration-response relationships for ATP inhibition of Kir6.2/SUR2A-YS channels in the absence (open squares; $n = 6$) and presence (open circles; $n = 6$) of Mg^{2+}. Current in the presence of ATP (I) is expressed as a fraction of that in the absence of ATP (I_C). The lines are the best fit of Eq. 1 to the mean data: open squares, IC_{50} = 7 µM (close to the 10 µM reported for Kir6.2/SUR2A by Tammaro et al. [2006]), $h = 1.5$ (0 Mg^{2+}); open circles, IC_{50} = 30 µM (close to the 29 µM reported for Kir6.2/SUR2A by Reimann et al. [2000]), $h = 1.3$ (2 mM Mg^{2+}). Mean ± SEM.

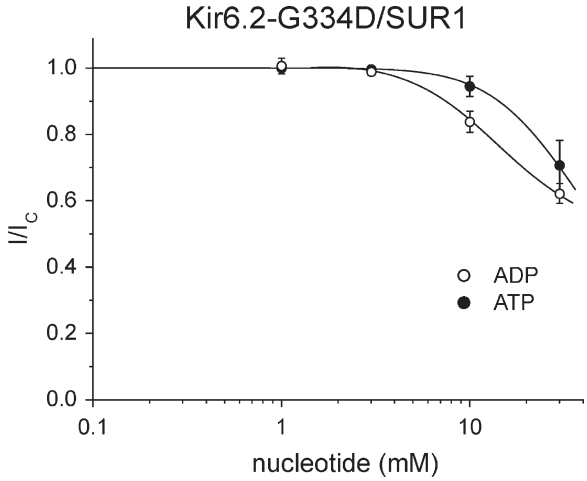

Figure S2. Concentration-response relationship for inhibition of Kir6.2-G334D/SUR1 channels by ATP ($n = 6$) and ADP ($n = 6$) in the absence of Mg^{2+}. Current in the presence of nucleotide (I) is expressed as a fraction of that in the absence of nucleotide (I_C). The lines are drawn by hand. Mean ± SEM.

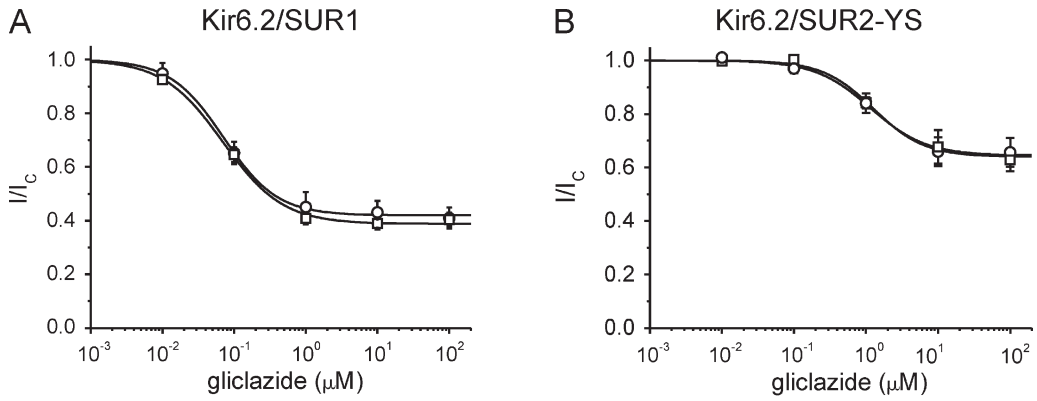

Figure S3. Concentration-response relationships for gliclazide inhibition of SUR1 and SUR2A-YS channels compared with either Kir6.2 or Kir6.2-G334D as the pore-forming subunit. (A and B) Concentration-response relationships for gliclazide inhibition of SUR1-containing (A; $n = 6$) and SUR2A-YS–containing (B; $n = 5$) channels. The pore-forming subunit was Kir6.2 (open circles) or Kir6.2-G334D (open squares). Current in the presence of gliclazide (I) is expressed as a fraction of that in the absence of gliclazide (I_C). The lines are the best fit of Eq. 1 to the mean data: $IC_{50} = 72$ nM, $h = 1.2$, $a = 0.42$ (A, open circles); $IC_{50} = 70$ nM, $h = 1.0$, $a = 0.39$ (A, open squares); $IC_{50} = 1.3$ μM, $h = 1.1$, $a = 0.65$ (B, open circles); $IC_{50} = 1.3$ μM, $h = 1.2$, $a = 0.64$ (B, open squares). Mean ± SEM.

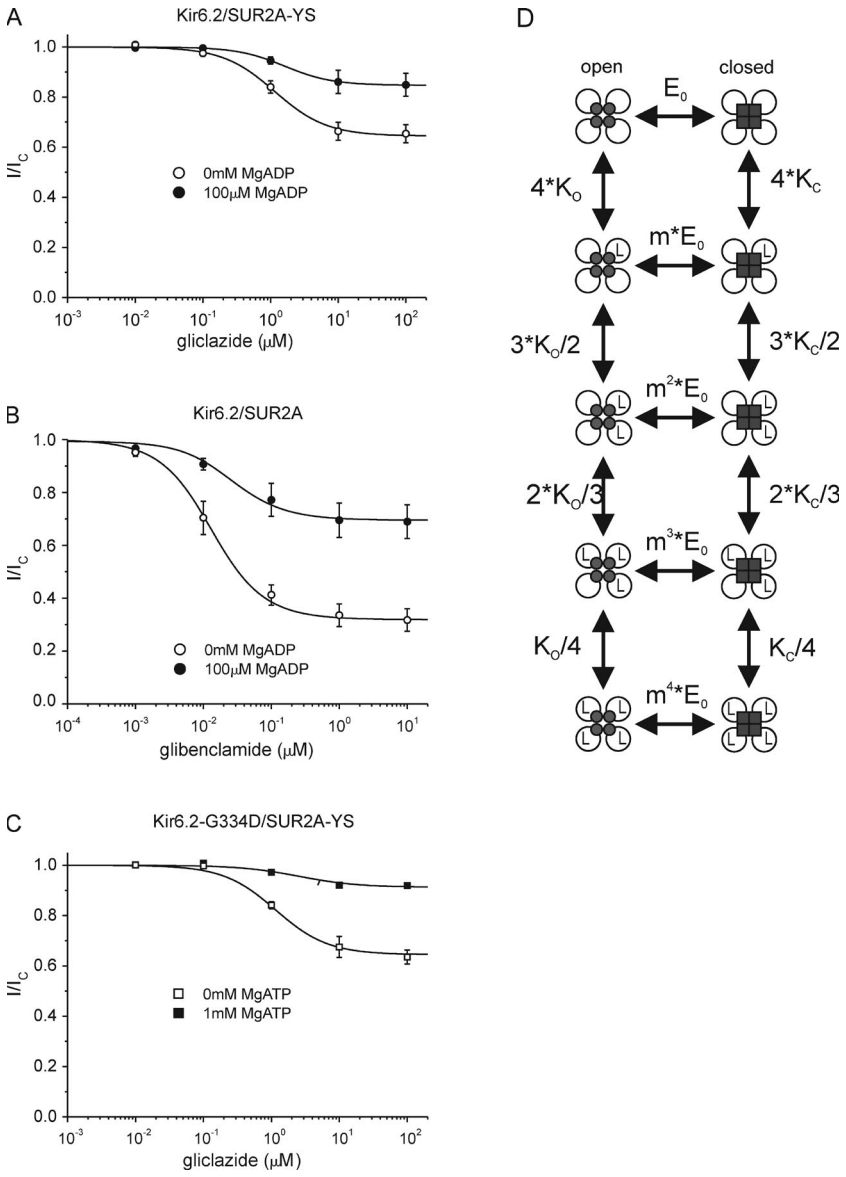

Figure S4. Simulation of concentration-inhibition relationships for sulfonylurea inhibition of SUR2A-containing channels using an MWC model. (A–D) Simulations of the concentration-response relationships for gliclazide inhibition of Kir6.2/SUR2A-YS (A) and Kir6.2-G334D/SUR2A-YS (C) channels and for glibenclamide inhibition of Kir6.2/SUR2A (B) channels in the absence and presence of 100 μM MgADP (A and B) and 1 mM MgATP (C) using a MWC model (D). The data are taken from Fig. 3 (B and D) (A and B, open circles), Fig. 5 B (A, closed circles), Fig. 5 D (B, closed circles), and Fig. 5 F (C, closed squares). The lines are the best fit to the mean data of Eq. S1:

$$\frac{I}{I_O} = \frac{\frac{\left(1 + K_O * [S]\right)^4}{\left(1+F\right) * \left(1 + K_O * [S]\right)^4 + E * \left(1 + K_O * m * [S]\right)^4}}{\frac{1}{1+F+E}}, \qquad \text{(S1)}$$

where I and I_O are the current in the presence and absence of the drug, respectively; $[S]$ is the sulfonylurea concentration, E and F (F = 0.16) are the equilibrium constants for slow and fast gating in the drug-free solution (Proks et al., 2013), and K_O and $K_C = m^*K_O$ are equilibrium binding constants for gliclazide to intraburst and interburst closed states, respectively. In the absence of nucleotides, the data are fitted with the MWC model assuming $P_O = 0.71$ (a value obtained experimentally for both Kir6.2/SUR2A-YS and Kir6.2/SUR2A channels: $P_O = 0.71 \pm 0.04$ [$n = 5$] and $P_O = 0.71 \pm 0.04$ [$n = 6$], respectively). This yields values of $K_O = 0.95$/μM and $K_C = 1.4$/μM for gliclazide and $K_O = 64$/μM and $K_C = 124$/μM for glibenclamide. The data in 100 μM MgADP (A) is best fitted with P_O of 0.79 (mean experimental value of $P_O = 0.79 \pm 0.02$; $n = 5$); the data in 1 mM MgATP (C) is best fitted with a P_O of 0.81 (mean experimental value of $P_O = 0.82 \pm 0.02$; $n = 5$), and the data in 100 μM MgADP (B) is best fitted with a P_O of 0.81 (mean experimental value of $P_O = 0.80 \pm 0.01$; $n = 5$). (D) MWC model for gating of K_{ATP} channels by ligands that bind to the sulfonylurea receptor. L, ligand (nucleotides or sulfonylureas); K_O and K_C, ligand-binding constants for the open and closed states, respectively; m, proportionality factor reflecting the change in the equilibrium gating constant E when the ligand is bound to the SUR ($m = K_C/K_O$). Mean ± SEM.

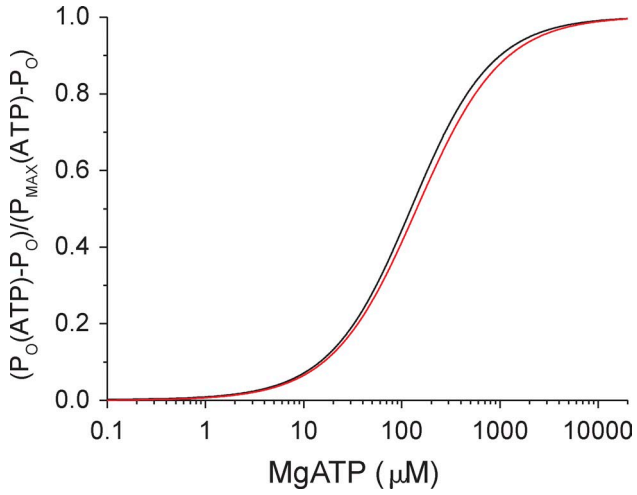

Figure S5. Effect of MgATP on the open probability of Kir6.2-G334D/SUR1 in the absence (black line) and presence of 30 µM gliclazide (red line), simulated using the MWC model (Fig. S4 D). The lines are drawn to Eq. S2:

$$\frac{P_O(ATP)-P_O}{P_{MAX}(ATP)-P_O} = \frac{\frac{(1+K_O*[ATP])^4}{(1+F)*(1+K_O*[ATP])^4+E*(1+K_O*m*[ATP])^4}-\frac{1}{1+F+E}}{\frac{1}{1+F+E*m^4}-\frac{1}{1+F+E}}, \quad \text{(S2)}$$

where $[ATP]$ is the ATP concentration, $P_O(ATP)$ is the open probability in the presence of ATP, $P_{MAX}(ATP)$ is the maximal open probability in the presence of ATP, K_O is the equilibrium binding constant for ATP to the open state, and F is the equilibrium gating constant for the fast gate (0.16; Proks et al., 2013). The factor m is given by $m = K_C/K_O$, where K_C is the equilibrium binding constant for ATP to the closed state and E is the equilibrium gating constant for the slow gate in the absence of the nucleotide (Proks et al., 2013). The value of K_O (0.00736/µM) was obtained from the fit to the experimental data using experimentally measured mean values of $P_O = 0.4$ and $P_{MAX}(ATP) = 0.71$. A transduction defect (such as that caused by gliclazide) will be represented in the MWC model by an increase in the factor m, which is given by $m = K_C/K_O$. When the experimental data were fit with the MWC model, the value of m increased from 0.66 in the absence of gliclazide to 0.90 in its presence (which is caused by the ~70% decrease in the maximal extent of channel activation; Fig. 7 D). For display purposes, the maximum increase in P_O in the presence of MgATP and gliclazide has been scaled to that in the presence of MgATP alone. The decrease in the efficacy of transduction (from nucleotide binding to channel opening) reduces the slope of the concentration-activation relationship only slightly. This in turn has only a mild effect on the value of the EC_{50} (the simulated EC_{50} increased from 120 to 140 µM in the absence and presence of the drug, respectively).

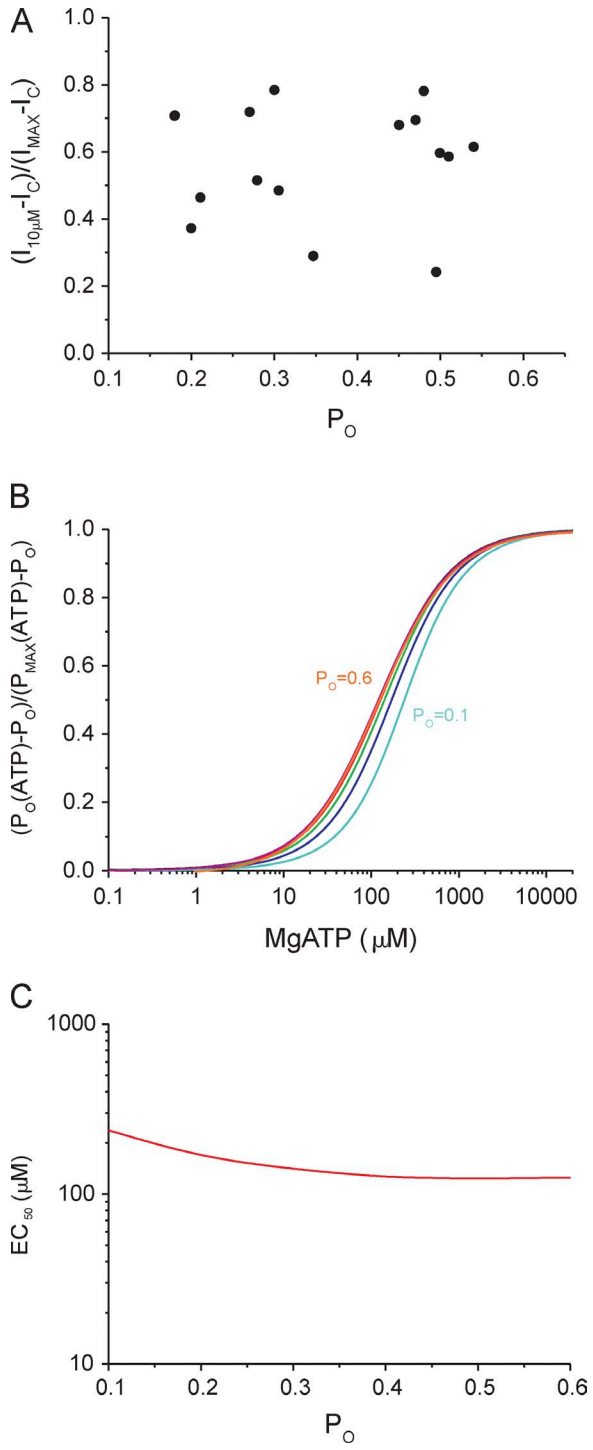

Figure S6. Effect of P_O on the EC_{50} for Mg-nucleotide activation of Kir6.2-G334D/SUR1 channels. (A) Relationship between the intrinsic P_O (i.e., that measured in nucleotide-free solution) and the fractional increase in Kir6.2-G334D/SUR1 current in the presence of 10 μM MgADP (i.e., a concentration which approximates the EC_{50} for MgADP activation). P_O was determined by noise analysis as described previously (Proks et al., 2010). Current is expressed as a fraction of the maximal current increase produced by MgADP (which occurs at 1 mM MgADP); i.e., $(I_{10\mu M} - I_C)/(I_{MAX} - I_C)$, where $I_{10\mu M}$ is the steady-state K_{ATP} current in the presence of 10 μM MgADP, I_C is the current in nucleotide-free solution obtained by averaging the current before and after nucleotide application, and I_{MAX} is the steady-state K_{ATP} current in the presence of 1 mM MgADP. (B) Concentration-activation relationships for MgATP, simulated with an MWC model (Fig. S4 D) for different values of intrinsic P_O (0.1, 0.2, 0.3, 0.4, 0.5, and 0.6). The lines are drawn to Eq. S2 (see Fig. S5). Values of *E* and *m* were calculated for different values of intrinsic P_O. (C) Values of EC_{50} for activation of Kir6.2-G334D/SUR1 channels by MgATP as a function of P_O (calculated using the MWC model used in B).

TABLE S1

Mean ± SEM values of P_O measured in nucleotide-free solution in the presence and absence of 2 mM Mg^{2+}

Channel	0 mM Mg^{2+}	2 mM Mg^{2+}
Kir6.2/SUR1	0.45 ± 0.03	0.43 ± 0.03
Kir6.2/SUR1-K1A	0.43 ± 0.03	0.43 ± 0.03
Kir6.2/SUR1-K2A	0.45 ± 0.05	0.46 ± 0.04
Kir6.2/SUR1-KAKA	0.48 ± 0.05	0.45 ± 0.07

P_O was determined by noise analysis, as described previously (Proks et al., 2010), after the fast rundown of channel activity (1 min after patch excision). $n = 11$ in all cases.

REFERENCES

Babenko, A.P. 2008. A novel ABCC8 (SUR1)-dependent mechanism of metabolism-excitation uncoupling. *J. Biol. Chem.* 283:8778–8782. http://dx.doi.org/10.1074/jbc.C700243200

Colquhoun, D. 1998. Binding, gating, affinity and efficacy: the interpretation of structure-activity relationships for agonists and of the effects of mutating receptors. *Br. J. Pharmacol.* 125:923–947. http://dx.doi.org/10.1038/sj.bjp.0702164

Craig, T.J., F.M. Ashcroft, and P. Proks. 2008. How ATP inhibits the open K_{ATP} channel. *J. Gen. Physiol.* 132:131–144. http://dx.doi.org/10.1085/jgp.200709874

Drain, P., X. Geng, and L. Li. 2004. Concerted gating mechanism underlying K_{ATP} channel inhibition by ATP. *Biophys. J.* 86:2101–2112. http://dx.doi.org/10.1016/S0006-3495(04)74269-1

Proks, P., H. de Wet, and F.M. Ashcroft. 2010. Activation of the K_{ATP} channel by Mg-nucleotide interaction with SUR1. *J. Gen. Physiol.* 136:389–405. http://dx.doi.org/10.1085/jgp.201010475

Proks, P., H. de Wet, and F.M. Ashcroft. 2013. Molecular mechanism of sulphonylurea block of $K_{(ATP)}$ channels carrying mutations that impair ATP inhibition and cause neonatal diabetes. *Diabetes.* 62:3909–3919. http://dx.doi.org/10.2337/db13-0531

Reimann, F., F.M. Gribble, and F.M. Ashcroft. 2000. Differential response of K(ATP) channels containing SUR2A or SUR2B subunits to nucleotides and pinacidil. *Mol. Pharmacol.* 58:1318–1325.

Tammaro, P., P. Proks, and F.M. Ashcroft. 2006. Functional effects of naturally occurring KCNJ11 mutations causing neonatal diabetes on cloned cardiac K_{ATP} channels. *J. Physiol.* 571:3–14. http://dx.doi.org/10.1113/jphysiol.2005.099168